
FungiTastic: A multi-modal dataset and benchmark for image categorization

Lukas Picek , Klára Janoušková , Milan Šulc , and Jiří Matas 

 University of West Bohemia & INRIA,  CTU in Prague, and  Second Foundation
 {lukaspicek, milansulc01}@gmail.com, {janouk11, matas}@fel.cvut.cz

Abstract

We introduce a new, challenging benchmark and a dataset, FungiTastic, based on fungal records continuously collected over a twenty-year span. The dataset is labeled and curated by experts and consists of about 350k multimodal observations of 5k fine-grained categories (species). The fungi observations include photographs and additional data, e.g., meteorological and climatic data, satellite images, and body part segmentation masks. FungiTastic is one of the few benchmarks that include a test set with DNA-sequenced ground truth of unprecedented label reliability. The benchmark is designed to support (i) standard closed-set classification, (ii) open-set classification, (iii) multi-modal classification, (iv) few-shot learning, (v) domain shift, and many more. We provide tailored baselines for many use cases, a multitude of ready-to-use pre-trained models on HuggingFace, and a framework for model training. A comprehensive documentation describing the dataset features and the baselines are available at GitHub and Kaggle.

1 Introduction

Biological problems provide a natural, challenging setting for benchmarking image classification methods [40, 51, 52]. Consider the following aspects inherently present in biological data. The species distribution is typically seasonal and influenced by external factors such as recent precipitation levels. Species categorization is fine-grained, with high intra-class and inter-class variance. The distribution is often long-tailed; for rare species, only a few samples are available. New species are being discovered, raising the need for the “unknown” class option. Commonly, the set of classes has a hierarchical structure, and different misclassifications may have very different costs. Think of mistaking a poisonous mushroom for an edible one, potentially lethal, and an edible mushroom for a poisonous one, which at worst means returning home with an empty basket. Similarly, needlessly administering anti-venom after making a wrong decision about a harmless snake bite may be unpleasant, but its consequences are incomparable to not acting after a venomous bite.

The properties of biological data listed above enable testing of, e.g., both open-set and closed-set categorization, robustness to prior and appearance domain shift, performance with limited training data, and dealing with non-standard losses. In contrast, most common benchmarks [10, 53] operate under the independent and identically distributed (i.i.d.) assumption, which is made valid by shuffling data and randomly splitting it for training and evaluation. In real-world applications, i.i.d data are rare since training data are collected well before deployment and everything changes over time [55].

Data sources play an important role in benchmarking [19, 21]. In the age of LLMs and VLMs trained on possibly the entirety of the internet at a certain point in time, access to new, “unseen” data is crucial to ensure methods are tested on data not indirectly “seen”, without knowing. Conveniently, many domains in nature are of interest to experts and the general public, who both provide a continuous stream of new and annotated data [39, 49]. The general public’s involvement introduces the problem of noisy training data; evaluating robustness to this phenomenon is also of practical importance.

Table 1: **Common image classification datasets** selected according to Google Scholar citations. We list suitability for closed-set classification (C), open-set classification (OS), few-shot (FS), segmentation (S), out-of-distribution (OOD) and multi-modal (MM) evaluation and modalities, e.g., images (I), metadata (M), and masks (S), available for training. The SOTA accuracy is limited to the classification task. $\forall = \{C, OS, FS, S, OOD, MM\}$

Dataset + citations (2022-24)	Classes	Training	Test	Modalities			Tasks	SOTA [†] Accuracy
				I	M	S		
Oxford-IIIT Pets [34]	1,060	37	1,846	3,669	✓	—	—	c 97.1 [13]
FGVC Aircraft [31]	1,190	102	6,732	3,468	✓	—	—	c 95.4 [2]
Stanford Dogs [26]	680	120	12,000	8580	✓	—	—	c 97.3 [2]
Stanford Cars [28]	2,060	196	8,144	8,041	✓	—	—	c 97.1 [29]
CUB-200-2011 [53]	1,910	200	5,994	5,794	✓	✓	✓	c 93.1 [7]
PlantNet300k [16]	30	1,081	243,916	31,112	✓	—	—	c 92.4 [16]
ImageNet-1k [10]	21,200	1,000	1,281,167	100,000	✓	—	—	C, FS 92.4 [12]
iNaturalist [52]	727	5,089	579,184	95,986	✓	—	—	C, FS 93.8 [46]
ImageNet-21k [42]	456	21,841	14,197,122	—	✓	—	—	C, FS 88.3 [46]
Insect-1M [32]	8	34,212	1,017,036	—	✓	✓	—	C, MM —
Species196 [20]	5	196	9,676	9,580	✓	✓	—	C, MM 88.7 [20]
NABirds [50]	283	555	48,562	—	✓	—	—	C, FS, MM 93.0 [11]
(our) DF20 [40]	42	1,604	266,344	29,594	✓	✓	—	c 80.5 [40]
(our) DF20-Mini [40]	42	182	32,753	3,640	✓	✓	—	c 75.9 [40]
FungiTastic	—	2,829	433,701	91,832	✓	✓	✓	\forall 75.3
FungiTastic-Mini	—	215	46,842	10,738	✓	✓	✓	\forall 74.8

Classification of data originating in nature, including images of birds [3, 53], plants [15, 18], snakes [6, 36], fungi [40, 52], and insects [17, 32] has widely been used for general benchmarking of machine learning algorithms, not just for fine-grained visual categorization. Most of the commonly used datasets are small for current standards; the number of classes is also limited. The performance is often saturated, reaching total accuracy between 85–95 %; see the rightmost column of Tab. 1. Typically, the datasets are solely image-based and focused on traditional image classification; few offer basic metadata attributes. Moreover, many popular datasets suffer from specific problems, e.g., regional, racial, and gender biases [48] and errors in labels [4, 50].

These limitations are particularly problematic for deployment, where machine learning models are expected to work with changing distributions and variable categories. As a result, the necessity of more comprehensive datasets that incorporate diverse modalities, reduce bias, and support more advanced learning paradigms, including multimodal, open-set, and few-shot classification, are becoming increasingly clear to better reflect the complexity of real-world data.

In the paper, we introduce **FungiTastic**, a comprehensive multi-modal dataset of fungi observations¹ which takes advantage of the favorable properties of natural data discussed above. The fungi observations include photographs, satellite images, meteorological data, segmentation masks, and location-related metadata. The *location metadata* enriches the observations with attributes such as the timestamp, GPS location, and information about the substrate and habitat. By incorporating various modalities, the dataset supports a robust benchmark for multi-modal classification, enabling the development and evaluation of sophisticated machine-learning models under realistic and dynamic conditions. **The key contributions of the proposed FungiTastic benchmark are:**

- It includes diverse data types, such as photographs, satellite images, bioclimatic time-series data, segmentation masks, and contextual metadata (e.g., timestamp, camera metadata, location, substrate, and habitat), offering a rich, multimodal benchmark.
- It addresses real-world challenges such as domain shifts, open-set problems, and few-shot classification, providing a realistic benchmark for developing robust machine learning models.
- The proposed benchmarks allow for addressing fundamental problems such as novel-class discovery, few-shot classification, and evaluation with non-standard cost functions.

¹A set of photographs and additional metadata describing one particular fungi specimen and surrounding environment. Usually, each photograph focuses on a different organ. For example observation, see Figure1

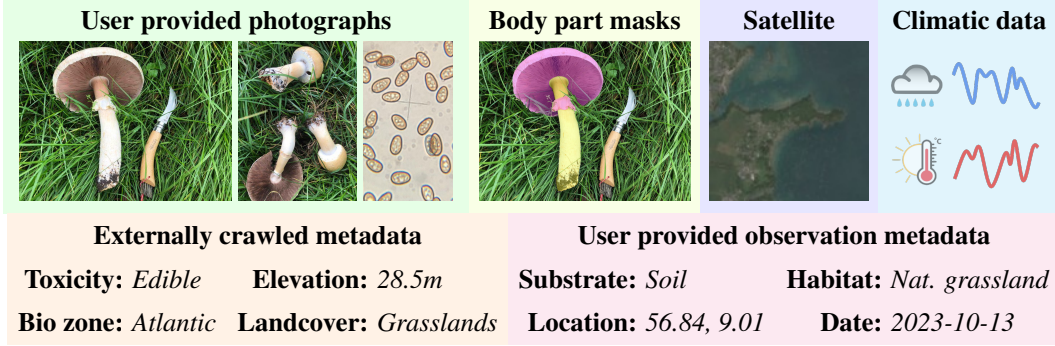


Figure 1: **A FungiTastic observation** includes one or more photographs of an *observed* specimen and usually also a microscopic image of its spores. For a subset ($\sim 70k$ photographs), we provide body part segmentation masks. The user-provided observation metadata is available for virtually all observations as well as additional crawled metadata. Geospatial data is available for all observations, DNA sequencing for a subset. Last but not least, we provide climatic time-series data.

2 The FungiTastic Benchmark

FungiTastic is built from fungi observations submitted to the Atlas of Danish Fungi before the end of 2023, which were labeled by taxon experts on a species level. In total, more than 350k observations consisting of 650k photographs collected over 20 years are used. Apart from the photographs, each observation includes additional observation data (see Figure 1) ranging from satellite images, meteorological data, and tabular metadata (e.g., timestamp, GPS location, and information about the substrate and habitat) to segmentation masks and toxicity status. The vast majority of observations got most of the attributes annotated. For more details about the attribute description and its acquisition process, see Subsection 2.1.

Since the data comes from a long-term conservation project, its seasonality and naturally shifting distribution make it suitable for time-based splitting. In this so-called **temporal division**, all data collected before a certain point is used for training, while data collected after that point is reserved for evaluation. Specifically, in our case, the **train** datasets consist of all observations up to the end of 2021, and the **val** and **test** datasets include all observations from 2022 and 2023, respectively.

The FungiTastic benchmark is designed to support not just standard closed-set classification but also (i) open-set classification, (ii) few-shot learning, (iii) multi-modal classification, (iv) domain shift, and many more. For the most common task, we provide a short description of curated subsets below and additional quantitative information about all the subsets in the Appendix in Table 6.

FungiTastic is a general subset that includes most of the observations (around 340k) and species (i.e., 2,829) alongside all the additional observation data except for the body part masks. As a bonus, we include a DNA-based test set of 725 species and 2,041 observations. The FungiTastic comes along with dedicated validation and test sets specifically designed for closed-set and open-set scenarios. While the closed-set validation and test sets only include species present in the training set, the open-set also includes observations with species that were observed only after 2022 and 2023, i.e., species not available in the training set. All the species (i.e., categories) with no examples in the training set are labeled as "unknown".

FungiTastic-Mini is a compact and challenging subset of the **FungiTastic** dataset designed primarily for prototyping and consisting of all observations belonging to 6 hand-picked genera (e.g., *Russula*, *Boletus*, *Amanita*, *Clitocybe*, *Agaricus*, and *Mycena*)². This subset comprises 46,842 images (25,786 observations) of 215 species, greatly reducing the computational requirements for training.

FungiTastic-FS subset, FS for few-shot, is formed by species with less than 5 observations in the training set, which were removed from the main (FungiTastic) dataset. The subset contains 4,293 observations encompassing 7,819 images of a total of 2,427 species. As in the FungiTastic data, the split into validation and testing is done according to the year of acquisition.

²These genera produce fruiting bodies of the toadstool type, which include many visually similar species and are of significant interest to humans due to their common use in gastronomy.

2.1 Additional Observation Data

This section provides a comprehensive overview of the accompanying data available alongside the user-submitted photographs. For each subset, we describe the data itself and, if needed, its acquisition process as well. Below, we describe **(i) tabular metadata**, which include key environmental attributes and taxonomic information accompanying nearly all image observations, **(ii) remote sensing data** at fine-resolution geospatial scale for each observation site, **(iii) meteorological data**, which provides long-term climate variables, and **(iv) body part segmentation masks** that delineate specific morphological features of fungi fruiting bodies, such as caps, gills, pores, rings, and stems. All those metadata are integral to advancing research combining visual, textual, environmental, and taxonomic information.

Multi-band remote sensing data such as satellite images offer detailed and globally consistent environmental information at a fine resolution, making it a valuable resource for species categorization (i.e., identification) [44, 35]. To allow testing the potential of such data and to facilitate easy use of geospatial data, we provide multi-band (e.g., R, G, B, NIR, and elevation) satellite patches with 128×128 pixel resolution (10m spatial resolution per pixel for R, G, B, and NIR, and 30m for elevation), centered on observation location. The data were extracted from rasters publicly available at Ecodatacube and ASTER Global Digital Elevation Model. While the extraction of the elevation data is straightforward, the raw pixel values in the Sentinel-2A rasters available on Ecodatacube might include extreme values. Therefore, we had to post-process raw data further to be in a standardized and expected form (i.e., an image with [0, 255] values). First, we clipped the values at 10,000. Next, the values were rescaled to a [0, 1] range and adjusted with a gamma correction factor of 2.5 (i.e., the values were raised to the power of 1/2.5). At last, the values were rounded and rescaled to [0, 255].



Figure 2: **Satellite images**. RGB images with a 128×128 resolution extracted from Sentinel2 data.

Body part segmentation masks of fungi fruiting body is essential for accurate identification and classification [9]. These morphological features provide crucial taxonomic information distinguishing some visually similar species. Therefore, we provide human-verified instance segmentation masks for all photographs in the FungiTastic–Mini (FungiTastic–M). We consider various semantic categories such as caps, gills, pores, rings, stems, etc. These annotations are expected to drive advances in interpretable recognition methods [43] and evaluation [22], with masks also enabling instance segmentation for separate foreground and background modeling [5]. All segmentation mask annotations were semi-automatically generated in CVAT using the Segment Anything Model [27].



Figure 3: **Fruiting body part segmentation**. We consider cap, gills, stem, pores, and ring.

Location-related metadata is provided for approximately 99.9% of the observations and describes the location, time, taxonomy and toxicity of the specimen, surrounding environment, and capturing device. See Table 2.1 for a detailed description of all available location-related metadata. While part of the metadata is usually provided by citizen scientists³ some attributes (e.g., elevation, land cover, and biogeographical) are crawled externally; all with a great potential to improve the classification accuracy and enable research on combining visual data with metadata.

³A member of the public who actively participates in scientific research and data collection, contributing valuable information and observations to support professional scientists.

Table 2: **List of available location-related metadata.** For a predominant number of observations, we provide a comprehensive set of data describing the surroundings or the specimen itself. Using such metadata for species identification allows to improve accuracy; see [11, 40].

Metadata	Description
Date of observation	Date when the specimen was observed in a format yyyy-mm-dd. Besides, we provide three additional columns with pre-extracted <i>year</i> , <i>month</i> , and <i>day</i> values.
EXIF	Camera device attributes extracted from the image, e.g., metering mode, color space, device type, exposure time, and shutter speed.
Habitat	The environment where the specimen was observed. Selected from 32 values such as Mixed woodland, Deciduous woodland, etc.
Substrate	The natural substance on which the specimen lives. A total of 32 values such as Bark, Soil, Stone, etc.
Taxonomic labels	For each observation, we provide full taxonomic labels that include all ranks from species level up to kingdom. All are available in separate columns.
Toxicity status	Whether is the species toxic or no. Since non-edible species can cause serious health issues as well, we include them as poisonous.
Location	Location data are provided in various formats, all upscaled from decimal GPS coordinates. Besides the latitude and longitude, we also provide administrative divisions for regions, districts, and countries.
Biogeographical zone	One of the major biogeographical zones, e.g., Atlantic, Continental, Alpine, Mediterranean, and Boreal.
Elevation	Standardized elevation value, i.e., height above the sea level.
Landcover	A land cover classification encodings including values such as savanna, barren, etc. Taken from MODIS Terra+Aqua [14].

Meteorological data and other climatic variables are vital assets for species identification and distribution modeling [1, 23]. In light of that, we provide 20 years of historical time-series monthly values of mean, minimum, and maximum temperature and total precipitation for all observations (see Figure 4 for example data). For each observation site, 20 years of data was extracted; for instance, an observation from the year 2000 includes data from 1980 to 2000. However, as the available climatic rasters only extend up to the year 2020, observations from 2020 to 2024 have missing values for those years not covered by existing data. In addition, we also provide 19 bioclimatic variables (related to temperature, seasonality, etc.) averaged over the period from 1981 to 2010. All data were extracted from climatic rasters available at CHELSA [25, 24].

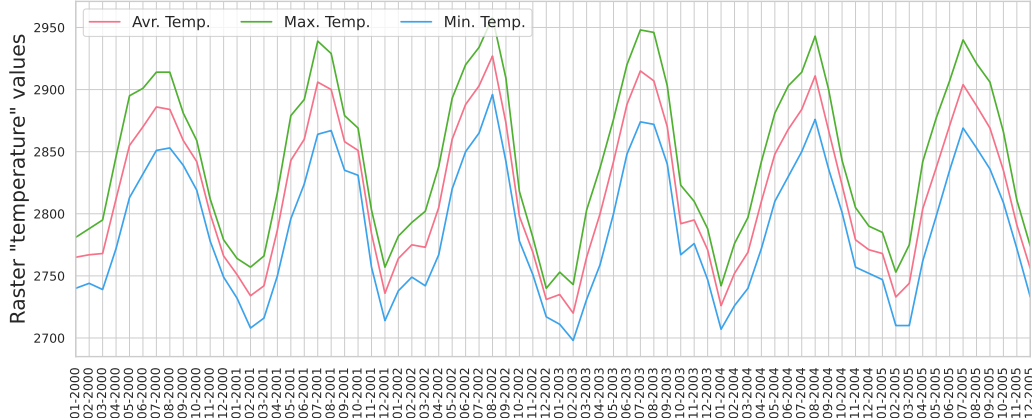


Figure 4: **Sample of available temperature data.** First 5 years (out of 20 available years) of average, maximum, and minimum monthly temperatures for a randomly selected location.

3 FungiTastic Benchmarks

The diversity and unique features of the FungiTastic dataset allow for the evaluation of various fundamental computer vision and machine learning problems. We present several distinct benchmarks, each with its own evaluation protocol. This section provides a detailed description of each challenge and the corresponding evaluation metrics. Metrics are further defined in Appendix A.

Closed-set classification: The FungiTastic dataset is a challenging dataset with many visually similar species, heavy long-tailed distribution, and considerable distribution shifts over time. Since the fine-grained close-set classification methodology is well-defined, we follow the widely accepted standard, and we, apart from accuracy, use the macro-averaged F1-score (F_1^m).

Open-set classification: In the Atlas of Danish Fungi (our data source), new species are continuously added to the database, including previously unreported species. This ongoing data acquisition enables a yearly data split with a natural class distribution shift (see Figure 5), and many species in the test data are absent in the training set. We follow a widely accepted methodology, and we propose an AUC as the main metric. Besides, we calculate F_1^m for two classes: "unknown" and "known."

Few-shot classification: All the categories with less than five samples in the FungiTastic, usually uncommon and rare species, form the few-shot subset. Being capable of recognizing those is of high interest to the expert. Since the few-shot dataset has no severe class imbalance like the other FungiTastic subsets, this benchmark’s main metric is top-1 accuracy. The F-1 score and top-k total accuracy are also reported. This challenge does not have any "unknown" category.

Chronological classification: Each observation in the FungiTastic (FungiTastic) dataset has a timestamp, allowing the study of species distribution changes over time. Fungi distribution is seasonal and influenced by weather, such as recent precipitation. New locations may be added over time, providing a real-world benchmark for domain adaptation methods, including online, continual, and test-time adaptation. The test dataset consists of fungi images ordered chronologically, meaning a model processing an observation at time t can access all observations with timestamps $t' < t$.

Classification beyond 0–1 loss function: Evaluation of classification networks is typically based on the 0–1 loss function, such as the mean accuracy, which applies to the metrics defined for the previous challenges as well. In practice, this often falls short of the desired metric since not all errors are equal. In this challenge, we define two practical scenarios: In the first scenario, confusing a poisonous species for an edible one (false positive edible mushroom) incurs a much higher cost than that of a false positive poisonous mushroom prediction. In the second scenario, the cost of not recognizing that an image belongs to a new species should be higher.

Segmentation: While acquiring human-annotated ground-truth segmentation masks can be resource-intensive, segmentation plays a critical role in advanced recognition methods and evaluation protocols for fine-grained image classification [5, 43]. High-accuracy segmentation of fungal images not only supports such methods but also enables automated analyses, such as assessing relationships between species-specific morphological features and environmental factors. This facilitates deeper insights into ecological and morphological patterns across locations, enhancing both model robustness and biological relevance. FungiTastic is suitable for evaluating semantic segmentation with the standard mean intersection over union (mIoU) metric and instance segmentation with the average precision (AP) metric.

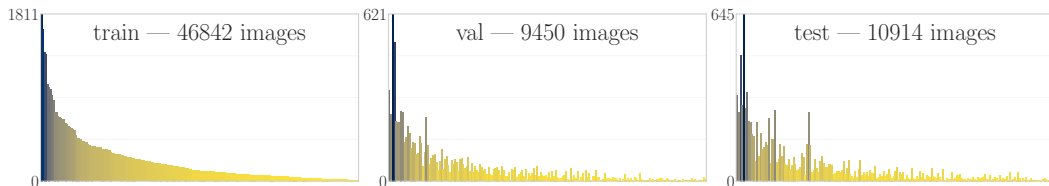


Figure 5: Class distribution shift on the FungiTastic-M dataset. The long-term data acquisition captures a phenomenon related to natural changes in species presence, i.e., class prior shift. Sorted in descending order based on their occurrence in the training set (color-coded to indicate relative frequencies in the training, validation, and test sets). The training set includes data from before 2022 (215 species), the validation set from 2022 (196 species), and the test set from 2023 (193 species).

4 Baseline Experiments

In this section, we provide a variety of weak and strong baselines based on state-of-the-art architectures and methods for three FungiTastic benchmarks. Below, we report results only for the closed-set, few-shot learning, and zero-shot segmentation, but other baselines will be provided later in the supplementary materials, in the documentation, or on the dataset website.

4.1 Closed-set image classification

We train a variety of state-of-the-art CNN architectures to establish some baselines for closed-set classification on the FungiTastic and FungiTastic-M. All selected architectures were optimized with Stochastic Gradient Descent with momentum set to 0.9, SeeSaw loss [54], a mini-batch size of 64, and Random Augment [8] with a magnitude of 0.2. The initial learning rate was set to 0.01 (except for ResNet and ResNeXt, where we used LR=0.1), and it was scheduled based on validation loss.

Results: Similarly to other fine-grained benchmarks, while the number of params, complexity of the model, and training time are more or less the same, the transformer-based architectures achieved considerably better performance on both FungiTastic and FungiTastic-M and two different input sizes (see Table 3). The best-performing model, BEiT-Base/p16, achieved F_1^m just around 40%, which shows the severe difficulty of the proposed benchmark.

Table 3: **Closed-set fine-grained classification FungiTastic and FungiTastic-M.** A set of selected state-of-the-art CNN- (top section) and Transformer-based (bottom section) architectures evaluated on the FungiTastic and FungiTastic-M test sets. All reported metrics show the challenging nature of the dataset. The best result for each metric is **highlighted**.

Architectures	FungiTastic-M – 224 ²			FungiTastic – 224 ²			FungiTastic-M – 384 ²			FungiTastic – 384 ²		
	Top1	Top3	F_1^m	Top1	Top3	F_1^m	Top1	Top3	F_1^m	Top1	Top3	F_1^m
ResNet-50	61.7	79.3	35.2	62.4	77.3	32.8	66.3	82.9	39.8	66.9	80.9	36.3
ResNeXt-50	62.3	79.6	36.0	63.6	78.3	33.8	67.0	84.0	39.9	68.1	81.9	37.5
EfficientNet-B3	61.9	79.2	36.0	64.8	79.4	34.7	67.4	82.8	40.5	68.2	81.9	37.2
EfficientNet-v2-B3	65.5	82.1	38.1	66.0	80.0	36.0	70.3	85.8	43.9	72.0	84.7	41.0
ConvNeXt-Base	66.9	84.0	41.0	67.1	81.3	36.4	70.2	85.7	43.9	70.7	83.8	39.6
ViT-Base/p16	68.0	84.9	39.9	69.7	82.8	38.6	73.9	87.8	46.3	74.9	86.3	43.9
Swin-Base/p4w12	69.2	85.0	42.2	69.3	82.5	38.2	72.9	87.0	47.1	74.3	86.3	43.3
BEiT-Base/p16	69.1	84.6	42.3	70.2	83.2	39.8	74.8	88.3	48.5	75.3	86.7	44.5

4.2 Few-shot image classification

Three baseline methods are implemented. The first baseline is standard classifier training with the Cross-Entropy (CE) loss. The other two baselines are nearest-neighbor classification and centroid prototype classification based on deep image embeddings extracted from large-scale pre-trained vision models, namely CLIP [41], BioCLIP [47] and DINOv2 [33].

Standard deep classifiers are trained with the CE loss to output the class probabilities for each input sample. Nearest neighbors classification (k-NN) constructs a database of training image embeddings. At test time, k nearest neighbors are retrieved, and the classification decision is made based on the majority class of the nearest neighbors. Nearest-centroid-prototype classification constructs a prototype embedding for each class by aggregating the training data embeddings of the given class. The classification is performed based on the image embedding similarity to the class prototypes. These methods are inspired by prototype networks proposed in [45].

Results: While DINOv2 [33] embeddings greatly outperform CLIP [41] embeddings, BioCLIP [47] (CLIP finetuned on biological data) outperforms them both, highlighting the dominance of domain-specific models. Further, the centroid-prototype classification always outperforms the nearest-neighbor methods in terms of accuracy, while the nearest-neighbor wins over the centroid-prototype in F-score. Finally, the best standard classification models trained on the in-domain few-shot dataset underperform both DINOv2 and BioCLIP embeddings in the F-score, which shows the power of methods tailored to the few-shot setup. For results summary, refer to Table 4.

Table 4: **Few shot classification on FungiTastic–Few-shot.** (Left) – Pretrained deep descriptors with the nearest centroid and 1-NN classification. All pre-trained models are based on the ViT-B architecture, CLIP, and BioCLIP with patch size 32 and DINOv2 with patch size 16. (Right) – Standard classification with cross-entropy-loss. Evaluated on the FungiTastic–Few-shot test set.

Model	Method	Top1	F_1^m	Top3	1^{shot}	2^{shot}	3^{shot}	4^{shot}	Architecture	Input	Top1	F_1^m	Top3
CLIP	1-NN	6.1	2.8	–	4.2	5.3	9.9	11.5	BEiT-B/p16	224×224	11.0	2.1	17.4
	centroid	7.2	2.2	13.0	3.6	7.4	12.5	12.5		384×384	11.4	2.1	18.4
DINOv2	1-NN	17.4	8.4	–	11.9	18.0	28.6	21.4	ConvNeXt-B	224×224	14.0	2.7	23.1
	centroid	17.9	5.9	27.8	12.2	17.8	23.4	31.6		384×384	15.4	2.9	23.6
BioCLIP	1-NN	18.8	9.1	–	12.8	21.3	30.0	29.4	ViT-B/p16	224×224	13.9	2.7	21.5
	centroid	21.8	6.8	32.6	12.7	23.5	32.9	40.3		384×384	19.5	3.7	29.0

4.3 Experiments with additional data

We provide baseline experiments using tabular metadata (habitat, month, substrate) based on our previous work [40]. The results in Table 5 show that all the attributes improve all the metrics. Individually, the addition of the habitat attribute results in the biggest gains (+2.27% of accuracy), followed by substrate (+1.15%) and month (+0.87%). Overall, habitat was the most efficient way to improve performance. With the combination of Habitat, Substrate, and Month, we improved the EfficientNet-B3 model’s performance on FungiTastic-Mini by 3.62%, 3.42% and 7.46% in Top1, Top3, and F1, respectively, indicating the gains are mostly orthogonal. Using the MetaSubstrate instead of Substrate resulted in performance lower by 0.2%, 0.5%, and 0.3% in Top1, Top3, and F1, respectively.

Table 5: **Ablation on a combination of selected observation-related metadata.** Utilizing a simple yet effective approach based on our previous work [40], we measure performance improvement using Habitat, Substrate, and Month and their combination. We also test how replacing Substrate with 31 variables for MetaSubstrate with nine variables with better interoperability to non-experts influences the performance. Evaluated with EfficientNet-B3 on FungiTastic-Mini test set.

<i>Habitat</i>	–	✓	–	–	–	✓	✓	✓	–	–	✓	✓	✓
<i>Month</i>	–	–	✓	–	–	✓	–	–	✓	✓	✓	✓	✓
<i>Substrate</i>	–	–	–	✓	–	–	✓	–	✓	–	✓	–	✓
<i>MetaSub.</i>	–	–	–	–	✓	–	–	✓	–	✓	–	✓	✓
Top1	69.5	+2.3	+0.9	+1.2	+0.9	+3.1	+3.0	+2.7	+1.9	+1.6	+3.6	+3.3	+3.5
F_1^m	43.5	+4.0	+1.1	+2.3	+1.5	+6.0	+5.9	+5.1	+4.0	+3.2	+7.5	+6.8	+7.3
Top3	85.4	+2.3	+0.5	+0.8	+0.6	+2.7	+2.9	+2.6	+1.5	+1.1	+3.4	+3.1	+3.4

4.4 Segmentation

A zero-shot baseline for foreground-background binary segmentation of fungi is evaluated on the FungiTastic–M dataset. The method consists of two steps: 1. The GroundingDINO [30] (the ‘tiny’ version of the model) zero-shot object detection model is prompted with the text ‘mushroom’ and outputs a set of instance-level bounding boxes. 2. The bounding boxes from the first step are used as prompts for the SAM [27] segmentation model. All the experiments are conducted on images with the longest edge resized to 300 pixels while preserving the aspect ratio.

Results: The baseline method achieved an average per-image IoU of 89.36%. While the model exhibits strong zero-shot performance, it sometimes fails to detect mushrooms. These instances often involve small mushrooms, where a higher input resolution could enhance detection, and atypical mushrooms, such as very thin ones. Another common issue is SAM’s tendency to miss mushroom stems. The results for the simplified foreground-background segmentation task (rather than instance-level semantic segmentation) underline the need for further development of domain-specific models. Qualitative results, including random images and examples where the segmentation performs best and worst, are reported in Figures 6, 7, and 8.



Figure 6: **Foreground-background segmentations on randomly selected FungiTastic-M photos.**
 Highlighted pixels correspond to: true positives, false positives, and false negatives.



Figure 7: **Foreground-background segmentations on FungiTastic-M with the highest IoU.**
 Highlighted pixels correspond to: true positives.



Figure 8: **Foreground-background segmentations on FungiTastic-M with the lowest IoU value.**
 Highlighted pixels correspond to: false positives and false negatives.

5 Conclusion

In this work, we introduced the FungiTastic, a comprehensive and multi-modal dataset and benchmark. The dataset includes a variety of data types, such as photographs, satellite images, climatic data, segmentation masks, and observation metadata. FungiTastic has many interesting features, which make it attractive to the broad machine-learning community. With its data sampling spanning 20 years, precise labels, rich metadata, long-tailed distribution, distribution shifts over time, the visual similarity between the categories, and multimodal nature, it is a unique addition to the existing benchmarks.

In the provided baseline experiments, we demonstrate how challenging the FungiTastic Benchmarks are. Even state-of-the-art architectures and methods yield modest F-scores of 39.8% in closed-set classification and 9.1% in few-shot learning, highlighting the dataset's difficulty compared to traditional benchmarks such as CUB-200-2011, Stanford Cars, and FGVC Aircraft. The proposed zero-shot baseline for the simplest segmentation task, binary segmentation of fungi fruiting body, achieved an average IoU of 89.36%, which still shows the potential for improvement in fine-grained visual segmentation of fungi.

Limitations mainly lie in the data collection process that influences data distribution. The majority of the data comes from Denmark, and further biases are potentially introduced by "sampling" in locations where certain species may be overrepresented due to their prevalence in frequently sampled areas or collector preferences. Additionally, not all meteorological data are available for every observation, which can affect of multi-modal classification approaches relying on such data.

Future work includes establishing continuous challenges to track progress across varied classification scenarios, expanding the set of weak and strong baselines, and including new test datasets for most benchmarks. Future efforts will also explore additional data, such as traits and textual descriptions of the species, to further improve the dataset's multi-modal capabilities.

Online Resources

The complexity and size of the dataset require hosting the dataset in multiple spaces. Since the *Kaggle dataset* is allowing to store datasets just up to around 140GB we provide images for the vanilla FungiTastic dataset in smaller resolution. The full-size images, as well as the Croissant metadata, are available for download through dataset documentation.

Apart from the dataset, we also provide a wide variety of assets. Notably, we provide:

- *FGVC*, a Pytorch-based framework designed for training deep learning classification models, hyperparameter fine-tuning, Weights&Biases logging, ONNX model export and HuggingFace deployment.
- *Sample notebooks* that allows loading pre-trained models, prediction and making submission on Kaggle benchmarks.
- All baseline *pre-trained models* available through the HuggingFace model hub allowing a straight-forward integration and usability.
- A comprehensive documentation with tables data samples and training strategies.

Acknowledgement

We extend our sincere gratitude to the mycologists from the Danish Mycological Society, particularly Jacob Heilmann-Clausen, Thomas Læssøe, Thomas Stjernegaard Jeppesen, Tobias Guldberg Frøslev, Ulrik Søchting, and Jens Henrik Petersen, for their invaluable contributions and expertise. We also thank the dedicated citizen scientists whose data and efforts have been instrumental to this project. Your support and collaboration have greatly enriched our work and made this research possible. Thank you for your commitment to advancing ecological understanding and conservation.

References

- [1] L. J. Beaumont, L. Hughes, and M. Poulsen. Predicting species distributions: use of climatic parameters in bioclim and its impact on predictions of species' current and future distributions. *Ecological modelling*, 186(2):251–270, 2005.
- [2] A. Bera, Z. Wharton, Y. Liu, N. Besis, and A. Behera. Sr-gnn: Spatial relation-aware graph neural network for fine-grained image categorization. *IEEE Transactions on Image Processing*, 31:6017–6031, 2022.
- [3] T. Berg, J. Liu, S. Woo Lee, M. L. Alexander, D. W. Jacobs, and P. N. Belhumeur. Birdsnap: Large-scale fine-grained visual categorization of birds. In *Proceedings of the IEEE conference on computer vision and pattern recognition*, pages 2011–2018, 2014.
- [4] L. Beyer, O. J. Hénaff, A. Kolesnikov, X. Zhai, and A. v. d. Oord. Are we done with imagenet? *arXiv preprint arXiv:2006.07159*, 2020.
- [5] G. Bhatt, D. Das, L. Sigal, and V. N Balasubramanian. Mitigating the effect of incidental correlations on part-based learning. *Advances in Neural Information Processing Systems*, 36, 2024.
- [6] I. Bolon, L. Picek, A. M. Durso, G. Alcoba, F. Chappuis, and R. Ruiz de Castañeda. An artificial intelligence model to identify snakes from across the world: Opportunities and challenges for global health and herpetology. *PLoS neglected tropical diseases*, 16(8):e0010647, 2022.
- [7] P.-Y. Chou, Y.-Y. Kao, and C.-H. Lin. Fine-grained visual classification with high-temperature refinement and background suppression. *arXiv preprint arXiv:2303.06442*, 2023.
- [8] E. D. Cubuk, B. Zoph, J. Shlens, and Q. V. Le. Randaugment: Practical automated data augmentation with a reduced search space. In *Proceedings of the IEEE/CVF conference on computer vision and pattern recognition workshops*, pages 702–703, 2020.
- [9] J. W. Deacon. *Fungal biology*. John Wiley & Sons, 2013.
- [10] J. Deng, W. Dong, R. Socher, L.-J. Li, K. Li, and L. Fei-Fei. Imagenet: A large-scale hierarchical image database. In *2009 IEEE conference on computer vision and pattern recognition*, pages 248–255. Ieee, 2009.
- [11] Q. Diao, Y. Jiang, B. Wen, J. Sun, and Z. Yuan. Metaformer: A unified meta framework for fine-grained recognition. *arXiv preprint arXiv:2203.02751*, 2022.
- [12] X. Dong, J. Bao, T. Zhang, D. Chen, W. Zhang, L. Yuan, D. Chen, F. Wen, N. Yu, and B. Guo. Peco: Perceptual codebook for bert pre-training of vision transformers. In *Proceedings of the AAAI Conference on Artificial Intelligence*, volume 37, pages 552–560, 2023.
- [13] P. Foret, A. Kleiner, H. Mobahi, and B. Neyshabur. Sharpness-aware minimization for efficiently improving generalization. *arXiv preprint arXiv:2010.01412*, 2020.
- [14] M. A. Friedl, D. Sulla-Menashe, B. Tan, A. Schneider, N. Ramankutty, A. Sibley, and X. Huang. Modis collection 5 global land cover: Algorithm refinements and characterization of new datasets. *Remote sensing of Environment*, 114(1):168–182, 2010.
- [15] C. Garcin, A. Joly, P. Bonnet, A. Affouard, J. Lombardo, M. Chouet, M. Servajean, T. Lorieul, and J. Salmon. Pl@ntNet-300K: a plant image dataset with high label ambiguity and a long-tailed distribution. In *NeurIPS Datasets and Benchmarks 2021*, 2021.
- [16] C. Garcin, A. Joly, P. Bonnet, J.-C. Lombardo, A. Affouard, M. Chouet, M. Servajean, T. Lorieul, and J. Salmon. Pl@ntnet-300k: a plant image dataset with high label ambiguity and a long-tailed distribution. In *NeurIPS 2021-35th Conference on Neural Information Processing Systems*, 2021.
- [17] Z. Gharaee, Z. Gong, N. Pellegrino, I. Zarubiieva, J. B. Haurum, S. Lowe, J. McKeown, C. Ho, J. McLeod, Y.-Y. Wei, et al. A step towards worldwide biodiversity assessment: The bioscan-1m insect dataset. *Advances in Neural Information Processing Systems*, 36, 2024.
- [18] H. Goeau, P. Bonnet, and A. Joly. Plant identification based on noisy web data: the amazing performance of deep learning (lifeclef 2017). *CEUR Workshop Proceedings*, 2017.
- [19] I. Goodfellow. *Deep learning*, volume 196. MIT press, 2016.

[20] W. He, K. Han, Y. Nie, C. Wang, and Y. Wang. Species196: A one-million semi-supervised dataset for fine-grained species recognition. *Advances in Neural Information Processing Systems*, 36, 2024.

[21] D. Hendrycks and T. Dietterich. Benchmarking neural network robustness to common corruptions and perturbations. *arXiv preprint arXiv:1903.12261*, 2019.

[22] R. Hesse, S. Schaub-Meyer, and S. Roth. Funnybirds: A synthetic vision dataset for a part-based analysis of explainable ai methods. In *Proceedings of the IEEE/CVF International Conference on Computer Vision (ICCV)*, pages 3981–3991, October 2023.

[23] R. J. Hijmans and C. H. Graham. The ability of climate envelope models to predict the effect of climate change on species distributions. *Global change biology*, 12(12):2272–2281, 2006.

[24] D. Karger, O. Conrad, J. Böhner, T. Kawohl, H. Kreft, R. Soria-Auza, N. Zimmermann, H. Linder, and M. Kessler. Climatologies at high resolution for the earth’s land surface areas. *sci. data* 4, 170122, 2017.

[25] D. N. Karger, O. Conrad, J. Böhner, T. Kawohl, H. Kreft, R. W. Soria-Auza, N. E. Zimmermann, H. P. Linder, and M. Kessler. Climatologies at high resolution for the earth’s land surface areas. *Scientific data*, 4(1):1–20, 2017.

[26] A. Khosla, N. Jayadevaprakash, B. Yao, and F.-F. Li. Novel dataset for fine-grained image categorization: Stanford dogs. In *Proc. CVPR workshop on fine-grained visual categorization (FGVC)*, volume 2. Citeseer, 2011.

[27] A. Kirillov, E. Mintun, N. Ravi, H. Mao, C. Rolland, L. Gustafson, T. Xiao, S. Whitehead, A. C. Berg, W.-Y. Lo, P. Dollar, and R. Girshick. Segment anything. In *Proceedings of the IEEE/CVF International Conference on Computer Vision (ICCV)*, pages 4015–4026, October 2023.

[28] J. Krause, M. Stark, J. Deng, and L. Fei-Fei. 3d object representations for fine-grained categorization. In *Proceedings of the IEEE international conference on computer vision workshops*, pages 554–561, 2013.

[29] D. Liu, L. Zhao, Y. Wang, and J. Kato. Learn from each other to classify better: Cross-layer mutual attention learning for fine-grained visual classification. *Pattern Recognition*, 140:109550, 2023.

[30] S. Liu, Z. Zeng, T. Ren, F. Li, H. Zhang, J. Yang, C. Li, J. Yang, H. Su, J. Zhu, et al. Grounding dino: Marrying dino with grounded pre-training for open-set object detection. *arXiv preprint arXiv:2303.05499*, 2023.

[31] S. Maji, E. Rahtu, J. Kannala, M. Blaschko, and A. Vedaldi. Fine-grained visual classification of aircraft. *arXiv preprint arXiv:1306.5151*, 2013.

[32] H.-Q. Nguyen, T.-D. Truong, X. B. Nguyen, A. Dowling, X. Li, and K. Luu. Insect-foundation: A foundation model and large-scale 1m dataset for visual insect understanding. In *Proceedings of the IEEE/CVF Conference on Computer Vision and Pattern Recognition*, pages 21945–21955, 2024.

[33] M. Oquab, T. Darcet, T. Moutakanni, H. Vo, M. Szafraniec, V. Khalidov, P. Fernandez, D. Haziza, F. Massa, A. El-Nouby, et al. Dinov2: Learning robust visual features without supervision. *arXiv preprint arXiv:2304.07193*, 2023.

[34] O. M. Parkhi, A. Vedaldi, A. Zisserman, and C. Jawahar. Cats and dogs. In *2012 IEEE conference on computer vision and pattern recognition*, pages 3498–3505. IEEE, 2012.

[35] L. Picek, C. Botella, M. Servajean, C. Leblanc, R. Palard, T. Larcher, B. Deneu, D. Marcos, P. Bonnet, and A. Joly. Geoplant: Spatial plant species prediction dataset. *arXiv preprint arXiv:2408.13928*, 2024.

[36] L. Picek, M. Hrúz, A. M. Durso, and I. Bolon. Overview of snakeclef 2022: Automated snake species identification on a global scale. 2022.

[37] L. Picek, M. Šulc, R. Chamidullin, and J. Matas. Overview of fungiclef 2023: fungi recognition beyond 1/0 cost. *Working Notes of CLEF*, 2023.

[38] L. Picek, M. Sulc, and J. Matas. Overview of fungiclef 2024: Revisiting fungi species recognition beyond 0-1 cost. *Working Notes of CLEF*, 2024.

[39] L. Picek, M. Šulc, J. Matas, J. Heilmann-Clausen, T. S. Jeppesen, and E. Lind. Automatic fungi recognition: deep learning meets mycology. *Sensors*, 22(2):633, 2022.

[40] L. Picek, M. Šulc, J. Matas, T. S. Jeppesen, J. Heilmann-Clausen, T. Læssøe, and T. Frøslev. Danish fungi 2020-not just another image recognition dataset. In *Proceedings of the IEEE/CVF Winter Conference on Applications of Computer Vision*, pages 1525–1535, 2022.

[41] A. Radford, J. W. Kim, C. Hallacy, A. Ramesh, G. Goh, S. Agarwal, G. Sastry, A. Askell, P. Mishkin, J. Clark, et al. Learning transferable visual models from natural language supervision. In *International conference on machine learning*, pages 8748–8763. PMLR, 2021.

[42] T. Ridnik, E. Ben-Baruch, A. Noy, and L. Zelnik-Manor. Imagenet-21k pretraining for the masses. *arXiv preprint arXiv:2104.10972*, 2021.

[43] M. Rigotti, C. Mikovic, I. Giurgiu, T. Gschwind, and P. Scotton. Attention-based interpretability with concept transformers. In *International conference on learning representations*, 2021.

[44] D. Rocchini, D. S. Boyd, J.-B. Féret, G. M. Foody, K. S. He, A. Lausch, H. Nagendra, M. Wegmann, and N. Pettorelli. Satellite remote sensing to monitor species diversity: Potential and pitfalls. *Remote Sensing in Ecology and Conservation*, 2(1):25–36, 2016.

[45] J. Snell, K. Swersky, and R. Zemel. Prototypical networks for few-shot learning. *Advances in neural information processing systems*, 30, 2017.

[46] S. Srivastava and G. Sharma. Omnivec: Learning robust representations with cross modal sharing. In *Proceedings of the IEEE/CVF Winter Conference on Applications of Computer Vision*, pages 1236–1248, 2024.

[47] S. Stevens, J. Wu, M. J. Thompson, E. G. Campolongo, C. H. Song, D. E. Carlyn, L. Dong, W. M. Dahdul, C. Stewart, T. Berger-Wolf, et al. Bioclip: A vision foundation model for the tree of life. In *Proceedings of the IEEE/CVF Conference on Computer Vision and Pattern Recognition*, pages 19412–19424, 2024.

[48] P. Stock and M. Cisse. Convnets and imagenet beyond accuracy: Understanding mistakes and uncovering biases. In *Proceedings of the European conference on computer vision (ECCV)*, pages 498–512, 2018.

[49] A. Swanson, M. Kosmala, C. Lintott, R. Simpson, A. Smith, and C. Packer. Snapshot serengeti, high-frequency annotated camera trap images of 40 mammalian species in an african savanna. *Scientific data*, 2(1):1–14, 2015.

[50] G. Van Horn, S. Branson, R. Farrell, S. Haber, J. Barry, P. Ipeirotis, P. Perona, and S. Belongie. Building a bird recognition app and large scale dataset with citizen scientists: The fine print in fine-grained dataset collection. In *Proceedings of the IEEE conference on computer vision and pattern recognition*, pages 595–604, 2015.

[51] G. Van Horn, E. Cole, S. Beery, K. Wilber, S. Belongie, and O. Mac Aodha. Benchmarking representation learning for natural world image collections. In *Proceedings of the IEEE/CVF conference on computer vision and pattern recognition*, pages 12884–12893, 2021.

[52] G. Van Horn, O. Mac Aodha, Y. Song, Y. Cui, C. Sun, A. Shepard, H. Adam, P. Perona, and S. Belongie. The inaturalist species classification and detection dataset. In *Proceedings of the IEEE conference on computer vision and pattern recognition*, pages 8769–8778, 2018.

[53] C. Wah, S. Branson, P. Welinder, P. Perona, and S. Belongie. The caltech-ucsd birds-200-2011 dataset. 2011.

[54] J. Wang, W. Zhang, Y. Zang, Y. Cao, J. Pang, T. Gong, K. Chen, Z. Liu, C. C. Loy, and D. Lin. Seesaw loss for long-tailed instance segmentation. In *Proceedings of the IEEE/CVF conference on computer vision and pattern recognition*, pages 9695–9704, 2021.

[55] Wikipedia. Heraclitus — Wikipedia, the free encyclopedia. <http://en.wikipedia.org/w/index.php?title=Heraclitus&oldid=1227413074>, 2024.

A Evaluation Metrics

A.1 Closed and open set classification

The main evaluation metric is F , the macro-averaged F1-score. For closed-set classification, the evaluation is standard, and for open-set, it is defined as

$$F = \frac{1}{C} \sum_{c=1}^C F_c, \quad F_c = \frac{2P_c \cdot R_c}{P_c + R_c}, \quad (1)$$

where P_c and R_c are the recall and precision of class c and C is the total number of classes, including the unknown class u .

The F1-score of the unknown-class, F^u , and the F-score over the known classes, F_k , are also of particular interest, with F_k defined as

$$F_K = \frac{1}{|K|} \sum_{c \in K} F_c, \quad (2)$$

where $K = \{1 \dots C\} \setminus \{u\}$ is the set of known classes. The F_K also corresponds to the main evaluation metric for standard closed-set classification. Additional metrics reported are top-1 and top-3 accuracy, defined as

$$Acc@k = \frac{1}{N} \sum_{i=1}^N \mathbf{1}(y_i \in q_k(x_i)), \quad (3)$$

where N is the total number of samples in the dataset, x_i, y_i are the i -th sample and its label and $q_k(x)$ are the top k predictions for sample x .

A.2 Classification beyond 0-1 loss function

For the classification beyond 0-1 cost, we follow the definition we set for the annual FungiCLEF competition [37, 38]. A metric of the following general form should be minimized.

$$\mathcal{L} = \frac{1}{N} \sum_{i=1}^N W(y_i, q_1(x_i)), \quad (4)$$

where N is the total number of samples, (x_i, y_i) are the i -th sample and its label, $q_1(x)$ is the top prediction for sample x and $W \in \mathbb{R}^{C \times C}$ is the cost matrix, C being the total number of classes. For the poisonous/edible species scenario, we define the cost matrix as

$$W^{p/e}(y, q_1(x)) = \begin{cases} 0 & \text{if } d(y) = d(q_1(x)) \\ c_p & \text{if } d(y) = 1 \text{ and } d(q_1(x)) = 0, \\ c_e & \text{otherwise} \end{cases} \quad (5)$$

where $d(y), y \in \mathcal{C}$ is a binary function that indicates dangerous (poisonous) species ($d(y) = 1$), $c_p = 100$ and $c_e = 1$. For the known/unknown species scenario, we define the cost matrix as

$$W^{k/u}(y, q_1(x)) = \begin{cases} 0 & \text{if } y = q_1(x) \\ c_u & \text{if } y = u \text{ and } q_1(x) \neq u, \\ c_k & \text{otherwise} \end{cases} \quad (6)$$

where $c_u = 10$ and $c_k = 1$.

B Supporting Figures and Tables

Table 6: **FungiTastic dataset splits – statistical overview.** We provide the number of observations, images, and classes for each benchmark and the corresponding dataset. "Unknown classes" are those with no available data in training. DNA stands for DNA-sequenced data.

Dataset	Subset	Observations	Images	Classes	Unknown classes	Metadata	Masks	Microscopic
FungiTastic – Closed Set	Train.	246,884	433,701	2,829	—	✓	—	✓
	Val.	45,616	89,659	2,306	—	✓	—	✓
	Test.	48,379	91,832	2,336	—	✓	—	✓
	DNA	2,041	5,117	725	—	✓	—	✓
FungiTastic–M – Closed Set	Train.	25,786	46,842	215	—	✓	✓	✓
	Val.	4,687	9,412	193	—	✓	✓	✓
	Test.	5,531	10,738	196	—	✓	✓	✓
	DNA	211	645	93	—	✓	✓	✓
FungiTastic–FS – Closed Set	Train.	4,293	7,819	2,427	—	✓	—	✓
	Val.	1,099	2,285	570	—	✓	—	✓
	Test.	998	1,909	566	—	✓	—	✓
FungiTastic – Open Set	Train.	246,884	433,701	2,829	—	✓	—	✓
	Val.	47,453	96,756	3,360	1,054	✓	—	✓
	Test.	50,085	97,551	3,349	1,013	✓	—	✓



Figure 9: **Additional samples of fruiting body part segmentation.**